ChemPubSoc Europe

DOI: 10.1002/cbic.201600494

CHEMBIOCHEM Full Papers

A Thioacetal Photocage Designed for Dual Release: Application in the Quantitation of Therapeutic Release by Synchronous Reporter Decaging

Pamela T. Wong,*[a, b] Shengzhuang Tang,[a, b] Jayme Cannon,[a, b] Jhindan Mukherjee,[a, b] Danielle Isham,[a] Kristina Gam,[a] Michael Payne,[a] Sean A. Yanik,[a] James R. Baker, Jr.,[a, b] and Seok Ki Choi*[a, b]

Despite the immense potential of existing photocaging technology, its application is limited by the paucity of advanced caging tools. Here, we report on the design of a novel thioacetal *ortho*-nitrobenzaldehyde (TNB) dual arm photocage that enabled control of the simultaneous release of two payloads linked to a single TNB unit. By using this cage, which was prepared in a single step from commercial 6-nitroverataldehyde, three drug–fluorophore conjugates were synthesized: Taxol-TNB-fluorescein, Taxol-TNB-coumarin, and doxorubicin-TNB-coumarin, and long-wavelength UVA light-triggered release experiments demonstrated that dual payload release occurred with rapid decay kinetics for each conjugate. In cell-based assays performed in vitro, dual release could also be controlled by UV exposure, resulting in increased cellular fluorescence and cytotoxicity with potency equal to that of unmodified drug towards the KB carcinoma cell line. The extent of such dual release was quantifiable by reporter fluorescence measured in situ and was found to correlate with the extent of cytotoxicity. Thus, this novel dual arm cage strategy provides a valuable tool that enables both active control and real-time monitoring of drug activation at the delivery site.

Introduction

Photocaging[1] has played an instrumental role in the spatiotemporal control of biological processes.[2] It is based on the temporary inactivation of a biologically active molecule through conjugation with a photocleavable protecting group (photocage), which can be conditionally removed by light exposure to reactivate the molecule (Scheme 1). The concept of photocaging has been extensively demonstrated in the control of cellular activities in vitro such as channel gating,[1] protein activation,[3] and gene regulation[2,4] as well as in the development of optogenetic animal models in vivo.[4b,c]

Protecting groups for photocaging are primarily composed of UV or visible light-responsive aromatic ring structures that include *ortho*-nitrobenzene (ONB),[1] nitro-benzofuran,[5] 6-bromo-7-hydroxycoumarin (BHC),[6] quinolone,[7] and cyanine.[8] Recently, the use of these cage molecules has been expanded to areas of controlled drug release, such as photopharmacology,[9] nanomedicine,[10] and image-guided drug transport.[11] In particular, the unique application of these molecules to the fluorescence-based imaging of intracellular prodrug activation[11e,f,12] is enabled by the multifunctional design capacity of the photocleavable cages, which allows for both a reporter fluorophore and a drug molecule to be attached to the same cleavable molecule. The spatially and temporally controlled release of both drug and imaging molecules within target cells allows for monitoring of the extent of drug release with a reporter readout in real-time.[11a–d] Of these cages, the ONB cage, which is the best characterized for its cleavage by one-photon[1] and two-photon[4b,5a,6a] absorption, has played a significant role in the advancement of controlled drug release.[2,13]

Despite its limited penetration through the skin (depth $\leq$ 0.2 mm),[14] long-wavelength UVA (315–400 nm) has the ability to reach as far as the subcutaneous layer. UVA is less toxic to most mammalian cells than shorter UVB and UVC, and thus has served as a tool for active control in chemical biology, such as in protein activation,[3a,5a,15] optogenetics,[4a,c,16] and in the photochemical internalization of bio-macromolecules.[17] More recently, applications of light-controlled mechanisms for drug release[13] have been developed by numerous laboratories, including ours, for the design of prodrugs and drug delivery systems for various therapeutic agents, including olaparib (AZD-2281),[11e] melphalan,[11f] methotrexate,[18] doxorubicin (Dox),[10b,c,19] paclitaxel (Taxol),[20] 5-fluorouracil,[21] tamoxi-

[a] Dr. P. T. Wong, S. Tang, J. Cannon, Dr. J. Mukherjee, D. Isham, K. Gam, M. Payne, S. A. Yanik, Dr. J. R. Baker, Jr., Dr. S. K. Choi
Michigan Nanotechnology Institute for Medicine and Biological Sciences
University of Michigan Medical School
1150 W. Medical Ctr. Drive, Ann Arbor, MI 48109 (USA)
E-mail: ptw@umich.edu
skchoi@umich.edu

[b] Dr. P. T. Wong, S. Tang, J. Cannon, Dr. J. Mukherjee, Dr. J. R. Baker, Jr., Dr. S. K. Choi
Department of Internal Medicine, University of Michigan Medical School
Ann Arbor, MI 48109 (USA)

Supporting information and the ORCID identification numbers for the authors of this article can be found under http://dx.doi.org/10.1002/cbic.201600494: details for compound synthesis, characterization, release kinetics, and cell studies.

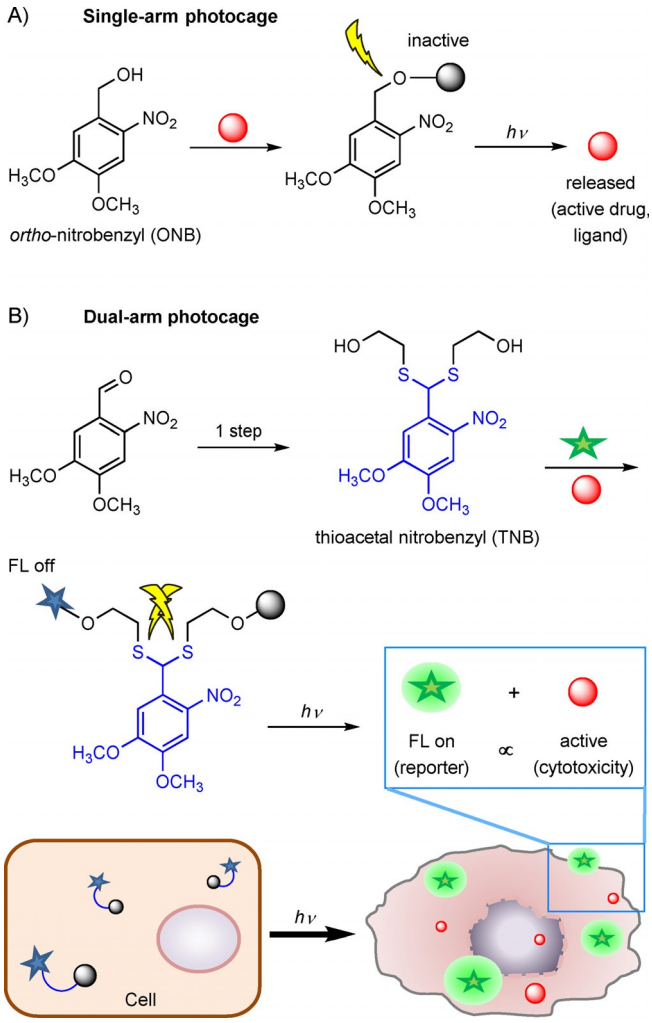

Scheme 1. A) The photocaging strategy, as illustrated with a conventional single arm photocage, *ortho*-nitrobenzyl (ONB); B) A dual arm strategy based on a thioacetal *ortho*-nitrobenzaldehyde (TNB) photocage that enables the synchronous release and activation of a fluorescent reporter probe (star) and a therapeutic molecule (sphere) upon triggering by light exposure. Illustration of its application for fluorescence (FL)-monitored cellular drug activation in vitro (below).

fen,[4a,8,16] and ciprofloxacin.[22] However, efficient implementation of photocage molecules for such applications[13] is often challenging, due in part to the synthetic complexity involved in drug and/or reporter conjugation, which requires a multistep process. Some of the applications involving nanoparticulate carrier systems required modification for presenting two attachable ends–one to the drug (or reporter probe), and the other to a particulate carrier.[10c,11a,19,21,23] The design of photocage molecules as linkers for non-particulate, small molecule applications is particularly difficult as compared to the carrier-based ones, as reflected by the scarcity of validated functional linkers.[11f,24] In addition, fewer photocage linkers have been implemented for the control of drug release[22–23] as compared to other types of linkers with release mechanisms triggered by cellular factors or conditions such as low pH,[13] reactive thiols,[11b,25] and metabolic enzymes.[11f,26]

In this study, we designed a dual-arm photocage molecule that provides both convenience in synthesis and payload conjugation and incorporates an externally controlled active release mechanism (Scheme 1 B). This photocage is based on a novel thioacetal *ortho*-nitrobenzaldehyde (TNB), which is cleaved in response to light exposure. This photocage strategy[24–25] allows for the active control of release, unlike other cleavable linkers that primarily rely on chemical and metabolic mechanisms that occur passively in response to cellular factors.[13] Here, we evaluated the practical application of this TNB cage for fluorescence-based monitoring of drug release by cross-tethering both an anticancer agent and a fluorescent probe to the cage. This dual conjugation strategy allows for light-controlled drug release and concomitant activation of the fluorescent reporter, which can be quantified in situ. As cellular cytotoxicity is directly correlated with the intracellular concentration of drug released, information regarding the efficiency of this release system can be obtained from the fluorescence readout. Thus, the intracellular kinetics and extent of drug release can be followed and measured on a real-time basis. This article reports on the design of three anticancer TNB reporter conjugates with proof of concept application validated for light-controlled drug release and real-time monitoring in cellular systems.

Results and Discussion

Rationale of TNB design

Despite extensive use, the ONB cage presents only a single cleavage site and is not optimal for dual arm, design which requires two attachment sites per cage. In order to address this design barrier and expand the applications of the ONB cage, we designed a TNB system in which the benzylic position is flanked by two identical arms, each connected with a C–S bond instead of a C–O bond (Scheme 2). Accordingly, each of the two arms has the potential for conjugation to a targeting ligand, drug, or reporter molecule, and has the ability to release the two payloads simultaneously by light-controlled cleavage of each C–S bond. This light control adds the benefit of selective payload release, as the thioacetal, which is often used as the protecting group for carbonyl compounds, is stable under a wide range of physiological conditions and is only susceptible to degradation under harsh synthetic conditions with oxidative or extremely acidic reagents.[27]

Synthesis of TNB cages

Two types of TNB photocages, **1** and **2** (Scheme 2), each terminated with a carboxylic acid or alcohol, respectively, were synthesized with 76–89% yield from commercial 6-nitroveratraldehyde and a requisite thiol (2.4 mol equiv) in a condensation reaction catalyzed by $BF_3{\cdot}Et_2O$ (1.2 mol equiv) and acetic acid (2.4 mol equiv) at ~0 °C (Schemes S2 and S3 in the Supporting Information): MS (ESI; *m/z*): **1** = 428.0 $[M+Na]^+$; **2** = 372.0 $[M+Na]^+$. This one-step synthetic methodology confers rapid access to various TNB photocages on a multigram scale. It is similarly applicable to other aromatic aldehyde precursors used in photocaging, such as 7-(diethylamino)coumarin-4-car-

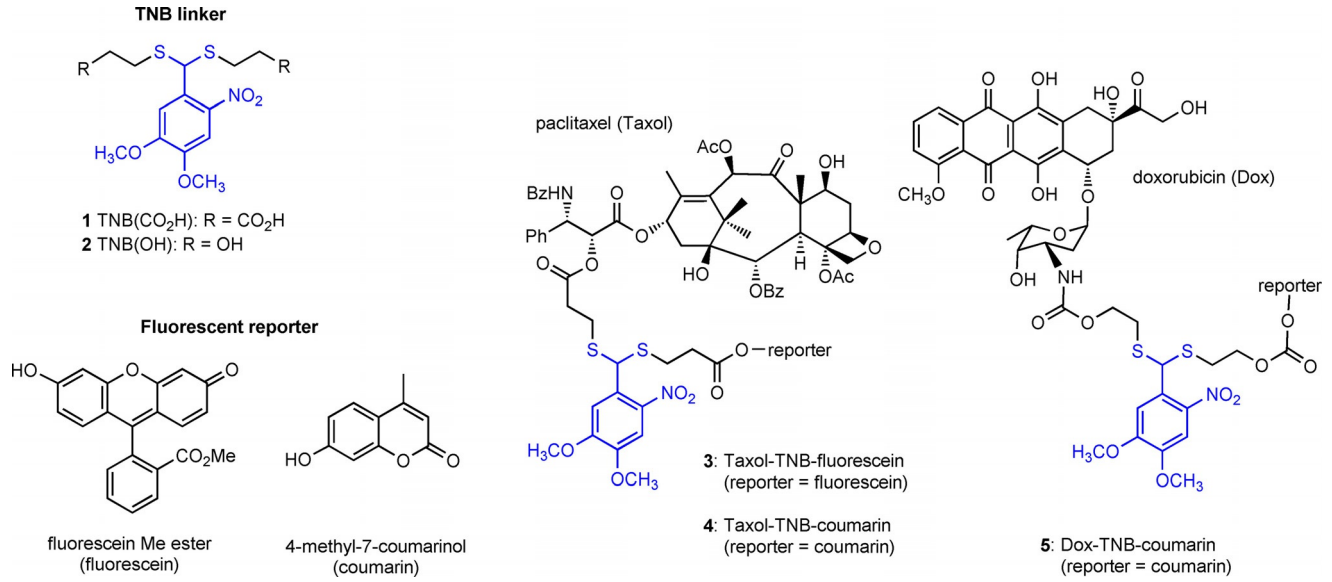

Scheme 2. Structures of TNB-based photocages **1** and **2** and three TNB-derived compounds (**3**–**5**) in which each TNB molecule serves as a branching spacer flanked by paclitaxel (Taxol) or doxorubicin (Dox) as a therapeutic molecule and a fluorescent reporter.

boxaldehyde, which was readily converted to its thioacetal form with 3-mercaptopropionic acid (not shown): MS (ESI; *m/z*): 462.0 $[M+Na]^+$, 440.0 $[M+H]^+$. In addition, each TNB photocage has a symmetric thioacetal, which provides equal reactivity in each of its two arms during dual payload conjugation.

Synthesis of TNB conjugates

We illustrate the synthetic convenience of this TNB cage strategy for dual payload conjugation by synthesizing three TNB conjugates, **3**–**5**. First, **1** TNB in which each arm is terminated with a carboxylic acid coupled with Taxol at its C2′-OH to prepare ester-based Taxol-TNB conjugate **6** (Scheme S2). The other carboxylic acid remaining in the intermediate was subsequently conjugated with a reporter probe, including fluorescein methyl ester (fluorescein) or 4-methyl-7-coumarinol (coumarin), through an ester linkage. This sequential reaction led to **3** (Taxol-TNB-fluorescein) and **4** (Taxol-TNB-coumarin), respectively, and each conjugate was fully characterized by mass spectrometry, ^{1}H NMR spectroscopy and fluorescence spectroscopy (Supporting Information): purity by analytical ultra-performance liquid chromatography (UPLC): ≥95% (**3**, **4**); ESI HRMS calcd for **3** ($C_{83}H_{80}N_2O_{25}S_2$): 1569.4564 $[M+H]^+$, found 1569.4542; calcd for **4** ($C_{72}H_{74}N_2O_{23}S_2$): 1399.4203 $[M+H]^+$, found 1399.4145; fluorescence spectroscopy **3**: λ_{ex} = 480 (±5) nm, λ_{em} = 520 (±5) nm; **4**: λ_{ex} = 365 nm, λ_{em} = 445 nm.

Second, **2** TNB, which is functionalized with an alcohol in its arm, was derivatized by coupling with 4-methyl-7-coumarinol through carbonate formation, then with Dox through a carbamate linkage, resulting in **5** (Dox-TNB-coumarin; Scheme S3). This TNB conjugate was characterized as above: analytical UPLC purity (≥95%); ESI HRMS calcd for **5** ($C_{52}H_{52}N_2O_{22}S_2$) 1138.2791 $[M+NH^4]^+$, found 1138.2777; fluorescence spectroscopy **5**: λ_{ex} = 365 nm, λ_{em} = 445 nm.

Photolysis of TNB cages

UV/visible absorption spectra of TNB cages **1** and **2** were measured in an aqueous medium (Figure 1). Each showed a λ_{max} at 346 nm (ε = 5,950 (**1**); ε = 4,292 (**2**) $M^{-1}cm^{-1}$), which is slightly longer than the λ_{max} value of 340 nm for a conventional ONB cage terminated with benzylic alcohol.[18b] This bathochromic shift might be attributable to the effect of the sulfur atom placed on the TNB cage, which is less electron withdrawing than the benzylic oxygen in the ONB system.[28] The photolysis of TNB cages **1** and **2** was performed by UVA exposure (365 nm), and its progress was monitored by ^{1}H NMR spectroscopy, UV/visible spectrometry, and UPLC, each providing evidence supportive of the cleavage mechanism proposed in Figure 1 A.

First, ^{1}H NMR analysis of photolysed **1** showed time-dependent disappearance of its benzylic proton (δ = 6.02 ppm) at the thioacetal group and concomitant growth of new aromatic signals in the upper field (Figure 1 B). This is indicative of oxidation of the thioacetal to 2-nitrosobenzoic thioester, which is believed to undergo subsequent hydrolysis to the 2-nitrosobenzoic acid and 3-mercaptopropionic acid (detected as an oxidized disulfide form; Figure S1). In addition to such hydrolytic cleavage, we anticipate that other types of chemical cleavage or ligation[29] might occur when it is cleaved in a cellular environment through reactions with amines and thiols. Second, UV/visible spectral traces acquired for each cage showed a rapid decrease in absorbance at the λ_{max} of each compound for light exposure times of up to 2 min (Figure 1 C), thus suggesting rapid photolytic cleavage of the TNB cage. The quantum yield ($\Phi_{uncaging}$) of uncaging was determined by ferrioxalate actinometry[30] for **1** and **2**, which showed 0.20 and 0.19, respectively, as summarized in Table S1. Such spectral and photophysical features were similarly observed in the photolysis of the comparable ONB cage ($\Phi_{uncaging}$ = 0.01–0.7).[6b] Third,

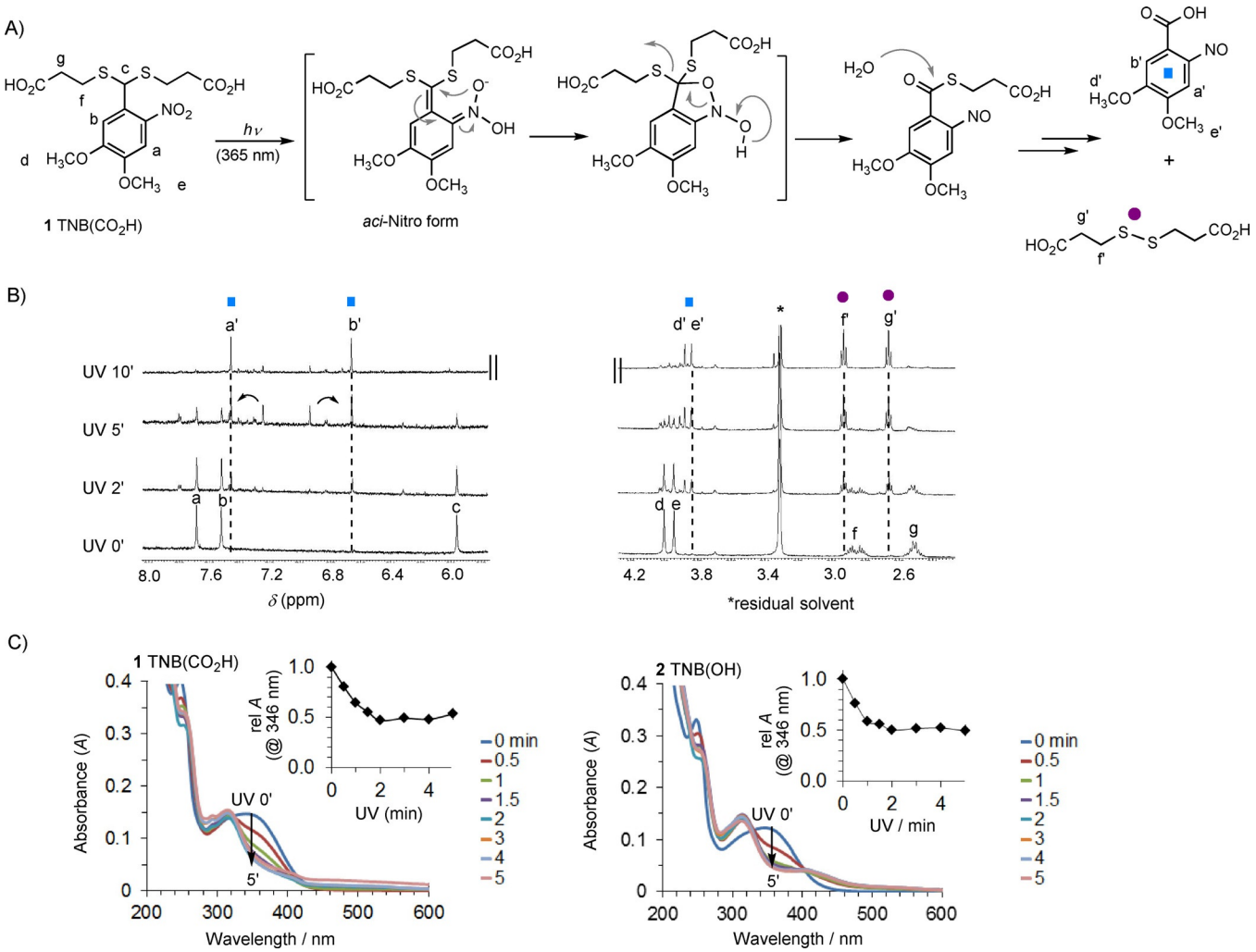

Figure 1. A) Proposed mechanism for the photolysis of **1** TNB(CO_2H) by long-wavelength UVA light (365 nm); B) ^1H NMR spectral traces (500 MHz) and proton assignment for the photolysis products of **1** (2.5 mM in 20% CD_3OD/D_2O); C) UV/Vis spectral traces for the photolysis of **1** and **2** ([**1**] = 25 μM; [**2**] = 29 μM, 10% aq. MeOH). Inset: plot of relative absorbance (*A*) at λ_{max} (346 nm) as a function of exposure time.

UPLC analysis for photolysed **1** showed the appearance of three new peaks, each at a shorter retention time (Figure S1), which is consistent with the formation of smaller molecular species, including the nitrosobenzoic acid and its (thio)esters. Collectively, these data point to the photocleavage of the TNB cage, yielding a 2-nitrosobenzoic acid product with the concomitant release of two thiol-terminated spacer molecules.

Light-controlled release kinetics

First, as a representative example, **3** (Taxol-TNB-fluorescein) in an aqueous solution (water/MeOH, 1:1) was exposed to UVA light (365 nm), and fluorescence spectra were measured (Figure 2). The emission intensities were compared at 520 nm (λ_{em} for fluorescein), showing an increase in emission as a function of exposure time (fourfold increase over a 10 min period). We attributed this fluorescence change to the release of fluorescein in its free phenolic form, which is characterized by stronger fluorescence emission than the unreleased conjugated form. The increase in fluorescence is consistent with the growth of an absorption peak at 485 nm (Figure S2B), which is indicative of fluorescein release. UPLC analysis was also performed with the photolysed solutions. Area under the curve (AUC) analyses indicated that the photolysis of **3** occurred rapidly in a time-dependent manner with a decay half-life ($t_{1/2}$) of <2 min and $\Phi_{uncaging}$ of 0.05 (Figure 2B). The UPLC analysis, in combination with LC-MS analysis, enabled detection of the release of two payloads, fluorescein and Taxol (Figure S2).

We believe that such dual release occurs through the proposed mechanisms described in Figure 2, in which a thiol-terminated precursor (C, D) is formed initially by light-triggered C–S bond cleavage, followed by intramolecular self-immolation,[11f,31] which leads to the release of the free payload species. This release mechanism can also produce two other intermediates (A, B), and these thiol ester-containing intermediates can then each be converted to the thiol-terminated precursor (C, D) through hydrolysis, transthioesterification,[29,32] or amidation[29] by water, thiols, amines, or other nucleophilic biomolecules in the cell. This mechanism was supported by the results of the LC-MS analysis performed for Taxol-TNB (a reference

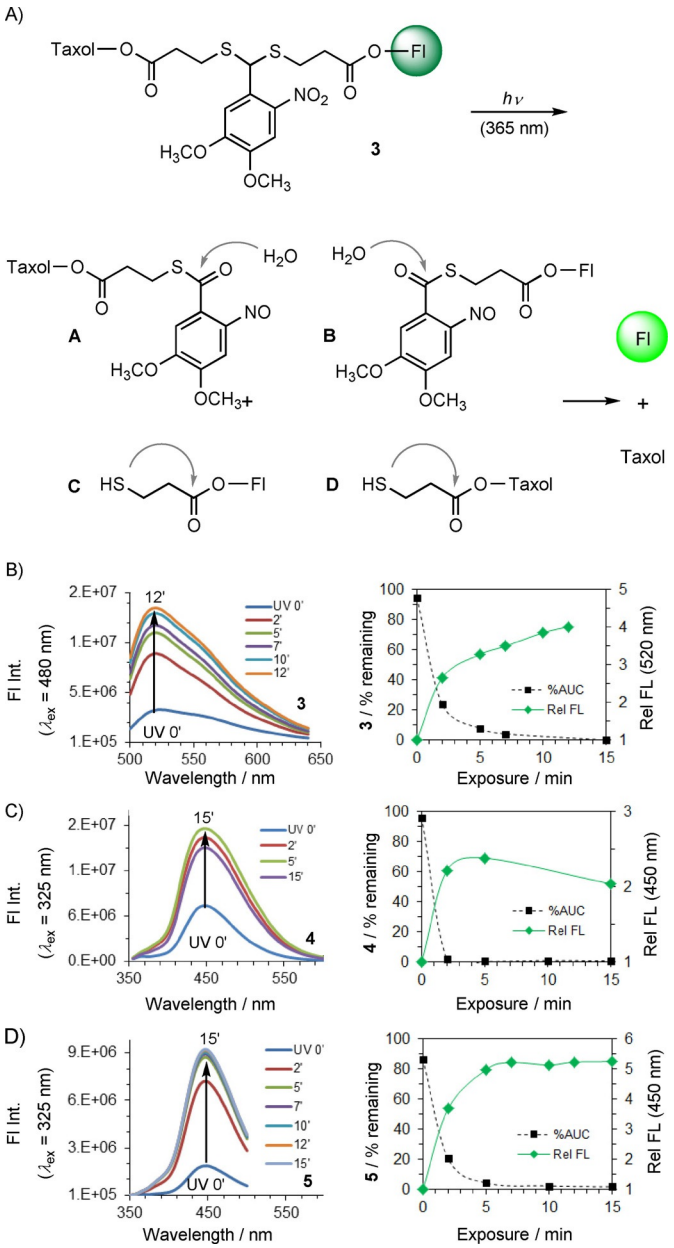

Figure 2. Photolysis of **3** (Taxol-TNB-fluorescein), **4** (Taxol-TNB-coumarin), and **5** (Dox-TNB-coumarin) in solution. A) Proposed mechanism for the light-mediated dual payload release for **3** and the structures of precursor compounds (A–D). B)–D) Release kinetics for **3**, **4**, and **5**, as monitored by fluorescence spectroscopy (left). Each plot (right) shows the remaining conjugate (% AUC by UPLC; left axis) and the fold increase in fluorescence (λ_{em} = 520 or 450 nm) relative to the non-UV-treated control of each conjugate (right axis) as a function of exposure time: [**3**] = 64 μM, [**4**] = 69 μM, and [**5**] = 62 μM.

compound without a linked reporter molecule) after 2 min of irradiation, which showed the release of precursor A along with Taxol (Figure S3). Our proposed mechanism for Taxol release from precursor D is also in agreement with the drug release from a thiol-terminated alkanoyl taxoid[33] (a homologue to the precursor D) by self-immolative cyclization, which was pioneered by Ojima, et al.[31a] and others[11c,34] using thiol-terminated prodrugs. However, despite the same mechanism, the rate of payload release from precursors C and D might be not identical, due to the difference in their leaving group capability. Thus, the release of fluorescein that occurs through a phenoxide anion (pK_a = 6.3–6.8)[35] could be faster than that of paclitaxel that occurs through an alkoxide anion ($pK_a > 10$). In summary, we believe that the present data, in combination with existing knowledge, are supportive of dual payload release by the self-immolative mechanism proposed here.

Light-controlled release studies were also performed with **4** (Taxol-TNB-coumarin) and **5** (Dox-TNB-coumarin), and photolysed solutions were characterized as summarized in Figure 2 and by UV/visible spectrometry and LC-MS analysis (Figures S4 and S5). Photolysis of these led to a 2.4- or 4.7-fold increase in fluorescence intensity, respectively, relative to the level before light exposure (Figure 2). This enhanced fluorescence occurred with the rapid disappearance of each TNB construct with decay half-lives ($t_{1/2}$) of < 2 min in UPLC analysis and $\Phi_{uncaging}$ of 0.07 (**4**) and 0.08 (**5**). The UV/visible spectra indicated exposure time-dependent rapid changes in absorption features. LC-MS analysis of selected photolysed solutions provided evidence supportive of the release of the free drug molecule and coumarin. We believe that this release also occurs through an intramolecular cyclization reaction involving an ester (**4**)[31a,33] or carbonate (**5**)[11c,34] bond by the nucleophilic terminal thiol on the drug or reporter precursor. It is notable that the quantum efficiency ($\Phi_{uncaging}$) of uncaging determined for each conjugate (**3**–**5**) showed a ~three- to fourfold decrease relative to its parent TNB cage, as presented above. This decrease could be attributable to photon absorption (such as a protective antenna effect[36]) by a conjugated payload molecule such as fluorescein, coumarin, or dox, given the significant molar absorptivity (ε) of these compounds at the irradiation (UVA) wavelength (Figures S2–S5).

Intracellular uptake and light-triggered release

To determine whether the TNB conjugates could be taken up intracellularly and subsequently cleaved through light activation after uptake, cellular fluorescence was analyzed by using flow cytometry. KB cells, an epithelial carcinoma line overexpressing folic acid receptor (FAR(+)), were used as a model system. Cells were incubated with 1.5 μM of **3** (Taxol-TNB-fluorescein) in folic acid-free cell culture medium for 0, 2, 6, and 24 h at 37 °C (Figure 3). At the end of the incubation period, unincorporated conjugate was removed by washing, and the cells were then exposed to long-wavelength UVA (365 nm) light for 2 min. For the incubation time of 0 h, the conjugate was added to the cells and immediately washed off prior to light exposure. Cellular fluorescein fluorescence (mean fluorescence intensity (MFI)) was then measured by flow cytometry. The percentage of cells with fluorescence greater than the intrinsic fluorescence of untreated cells was also determined (Figure 3C).

Taxol-TNB-fluorescein (**3**) was taken up intracellularly within 2 h of incubation, and continued to be taken up over 24 h, as evidenced by the slight increase in the cellular MFI and the percentage of cells with high fluorescence in the absence of

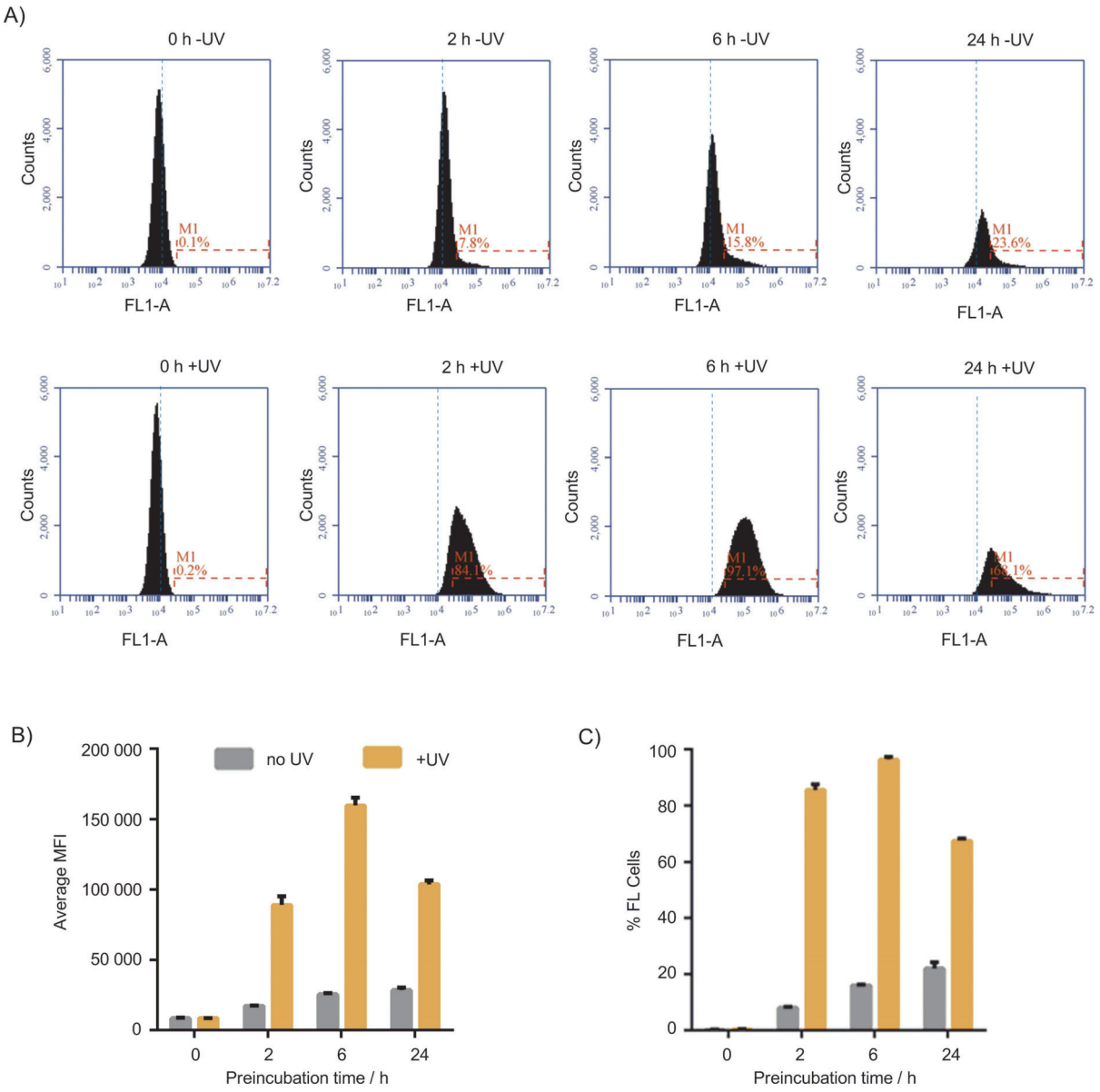

Figure 3. Determination of intracellular uptake by flow cytometry analysis. KB cells were incubated with 1.5 μM of **3** (Taxol-TNB-fluorescein) for the indicated times ($t = 0$, 2, 6, and 24 h), washed to remove extracellular conjugate, and then exposed to UVA (365 nm) for 2 min or left in the dark. Cell-associated fluorescence (fluorescein channel) was measured by flow cytometry. A) Representative histograms showing the distribution of fluorescence intensities for intact cells ± light exposure. B) Changes in the average cellular mean fluorescence intensity (MFI) for treated cells, and C) the percentage of cells with fluorescence (FL) higher than untreated cells.

light exposure, attributed to the fluorescence of the uncleaved conjugate (Figure 3C). Upon light exposure, a large increase in the cellular MFI and percentage of cells containing increased fluorescence was observed for cells incubated with **3** (e.g., 6.3-fold increase in MFI and 6.0-fold increase in the percentage of cells with increased fluorescence for cells treated with 1.5 μM of **3** with 6 h of incubation prior to light exposure). The increase in cellular fluorescence induced by light exposure increased in magnitude with longer preincubation times between 0–6 h, reflecting the intracellular accumulation of the conjugate (Figure 3B, C). These results confirm that a significant amount of the intact Taxol-TNB-fluorescein conjugate is taken up intracellularly and is retained within the cell in a relatively intact state that maintains the fluorescein reporter in a fluorescently quenched state. Furthermore, these results demonstrate that UV-mediated photocleavage of the TNB construct can occur intracellularly. The decrease in MFI and percentage of fluorescent cells between 6 and 24 h, however, is attributed to cell death due to the cytotoxic effects of the drug conjugate.

Correlation between fluorescence and cytotoxicity in vitro

To confirm the functional activity of the TNB conjugates and the released drug, their cytotoxic properties were evaluated in KB cells with or without exposure to UV. A microplate assay that allowed measurement of fluorescence on a real-time basis

in live cells, and measurement of the viability of the same cells by an XTT assay, was employed instead of the fluorimeter, which was used for photolysis in solution (Figure 2). FAR(+) KB cells were treated with **3**, **4**, and **5** at various concentrations and exposed briefly to UVA light (365 nm) for 2 min (Figure 4). The fluorescence of the reporter molecule was measured immediately. A large increase in either fluorescein or coumarin reporter fluorescence (several orders of magnitude) was seen for all three conjugates upon UV irradiation relative to treated cells that were not exposed to UV. Fluorescein and coumarin conjugates had similar low fluorescence emission intensities prior to light activation at their respective excitation and emission wavelengths. Interestingly, for the Taxol-TNB conjugates, the fluorescein-containing conjugate, **3**, displayed an increase in fluorescence of much greater magnitude compared to the coumarin conjugate, **4** (Figure 4A and B). This lower fluorescence exhibited by **4** might be explained, in part, by its lower increase in fluorescence in solution after UV exposure (Figure 2B and C).

The increase in reporter fluorescence upon light exposure correlated with the concomitant increase in cytotoxicity of the drug conjugates. Cytotoxicity displayed a dose dependency for both non-UV- and UV-treated cells. Prior to UV exposure, **3**, **4**, and **5** exhibited minimal cytotoxicity (IC_{50} values of 0.24, 0.23, and 9.22 μM, respectively) compared to unconjugated doxorubicin and Taxol (0.04, 0.02 μM, respectively; Figure S6), thus suggesting that conjugation might reduce systemic toxicity. Upon UV exposure, the cytotoxicity of the conjugates increased dramatically, decreasing the IC_{50} values by an order of magnitude (IC_{50} values for **3**, **4**, and **5**: 0.04, 0.05, and 0.84 μM, respectively). As controls, no effect of light exposure on cell viability or fluorescence intensity (inset) was observed for either free Taxol or doxorubicin, both of which were highly cytotoxic, even at low nanomolar concentrations (Figure S6). These results demonstrate the ability to actively control the cytotoxicity of these constructs temporally and support the utility of fluorescence readouts as a means for monitoring the amount of drug transported to the target cell and accordingly, for predicting tumor cell viability in situ.

Real-time release kinetics

The positive correlation observed between fluorescence and cytotoxicity above is supportive of the ability to exert spatiotemporal control on drug release and perform quantitative monitoring of the extent of release indirectly by using fluorescence measurements in real-time. In order to characterize the release kinetics in cellular systems, we determined the extent of additional reporter release (reflective of drug release), over time after the initial UV stimulus by following the increase in the fluorescence of live cells over 24 h of incubation at 37 °C (Figure 5). Incubation of cells treated with **3** or **4** and exposed to UV (exposure time = 0.5 or 2 min) led to a rapid increase in fluorescence within the first 3 h of incubation, followed by a small gradual increase over the remaining 24 h. The endpoint fluorescence after 24 h was more than twofold the fluorescence measured immediately after UV exposure. The continued release of reporter and drug for an extended period after the initial UV stimulus was not due to cleavage of the cage by cellular factors, but this slow gradual increase was likely due to

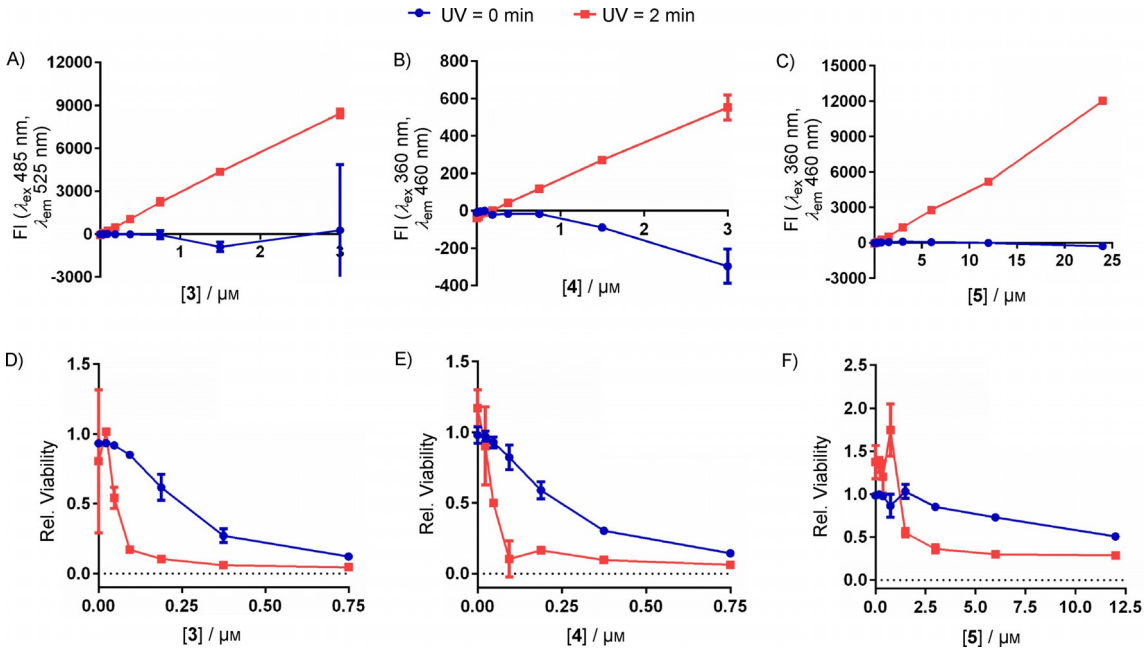

Figure 4. Fluorescence intensity (A–C) measured by a microplate reader and cell viability (D–F) of FAR(+) KB cells treated with **3**, **4**, or **5**, with or without exposure to long-wavelength UV (365 nm) for 2 min (UV = 0, 2 min). Fluorescence was measured at λ_{ex} = 485 nm, fluorescein release (**3**) at λ_{em} = 528 nm, and coumarin release (**4**, **5**) at λ_{ex} = 360 nm, λ_{em} = 460 nm immediately after the UV exposure period. Cell viability was measured by incubation of the cells treated with each conjugate for 24 h post UV exposure, and then washed and grown for four additional days prior to measuring the viability with an XTT assay relative to untreated cells.

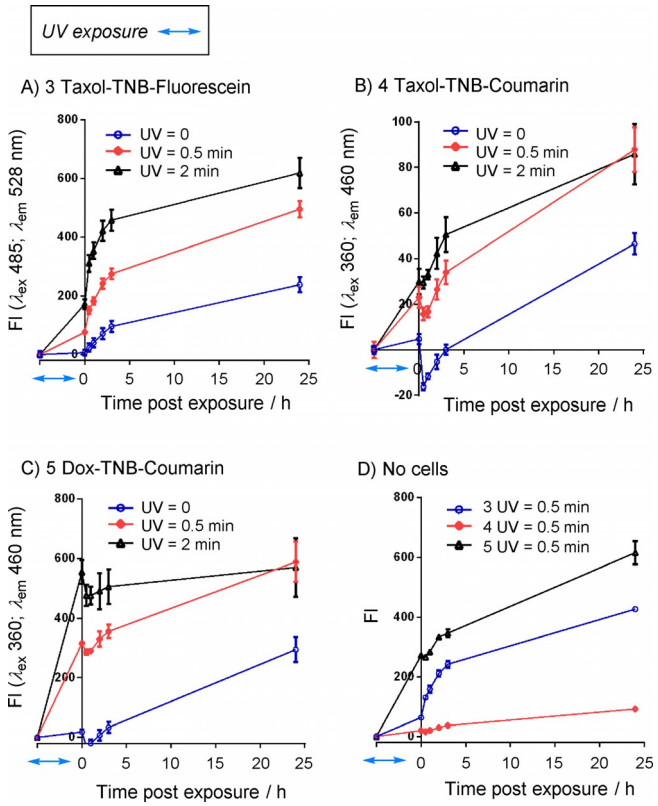

Figure 5. Real-time monitoring of reporter fluorescence intensities under three different exposure conditions. A)–C) The fluorescence of FAR(+) KB cells treated with **3** (Taxol-TNB-fluorescein), **4** (Taxol-TNB-coumarin), or **5** (Dox-TNB-coumarin), each at 1.5 μM, was monitored by using a microplate reader immediately after variable lengths of exposure to long-wavelength UVA light (365 nm; UV = 0, 0.5, 2 min; marked with a blue double arrow). Post exposure time = 0 h represents the fluorescence measured immediately after UV exposure. The cellular fluorescence was subsequently followed over the course of 24 h of additional incubation at 37 °C. D) The fluorescence intensities of TNB conjugates **3**, **4**, and **5** in medium alone were monitored at their respective excitation and emission wavelengths following 0.5 min of UV exposure.

the self-immolative conversion of transient dye intermediates to a fully fluorescent dye molecule, as similar release kinetics were observed in the cell-free control (Figure 5 D).

Interestingly, in contrast to conjugates **3** and **4**, conjugate **5** showed only a minimal additional increase in fluorescence over the course of 24 h following the initial jump in fluorescence immediately after 2 min of UV exposure. This suggests that 2 min of UV exposure was sufficient to rapidly and fully release all of the coumarin in **5**. Thus, dye release from light-exposed **5** is likely to occur faster than from **3** or **4**. We believe that such differences among the three TNB conjugates might be attributable to the mechanism and rate of the self-immolation reaction[11c,34] by which the fluorescent dye molecule is converted from its respective thiol precursor. The thiol precursor generated from **5** has a coumarin moiety attached to the spacer through a more chemically reactive carbonate functionality which is thus more labile to nucleophilic displacement reactions than the ester functionality present in the thiol precursors from **3** and **4**.

Control cells that were treated with the conjugates but were unexposed to UV showed only minimal changes in bulk reporter fluorescence over 3 h of incubation, indicating stability of **3**–**5** during the fluorescence measurement time period in the fluorescence assay in Figure 4 and confirming the role of UV irradiation in reporter activation. However, prolonged incubation for 24 h led to some increase in reporter fluorescence for conjugates **3**–**5**, even without light exposure, although the fluorescence at 24 h was still <30–50% that of the light exposed cells after 24 h. This "dark" release of reporter, and putatively of drug, accounts for the degree of cytotoxicity observed for the non-UV treated cells in Figure 4. This partial increase suggests the possibility of dye release by other non-photochemical pathways, including ones not triggered by cleavage of the C–S bond in the TNB cage, such as intermolecular nucleophilic attack at the carbonate or ester bond by water, free amines, and thiols. Involvement of these passive mechanisms might similarly occur in the release of the drug payload. In particular, TNB conjugates **3** and **4** each carry Taxol attached through an ester bond, which is reportedly labile and cleaved by hydrolysis and lysosomal enzymes.[31a,37] However, the stability of these constructs over several hours makes them functional over the time frame required for them to reach the target site for photoactivation applications.

In order to enhance our understanding of this non-photochemical background release, we investigated the effect of a model thiol, 3-mercaptopropionic acid (1 mM ± UV), on the release of coumarin by using TNB-coumarin as a model system (Figure S7). When added at a ~5 molar equivalent, the thiol lacked the ability to trigger the release of coumarin in the absence of UVA light exposure. In combination with light exposure, the thiol played a clear role in altering the distribution of thioester precursors and accordingly made an indirect contribution to the dye release. This result, though observed in a simple model system, was supportive of the earlier results observed in the cellular system (Figure 5). Lastly, intracellular esterase activity might contribute to the non-photochemical background release, as these esterases are well known for their role in the hydrolytic activation and intracellular trapping of cell-permeable fluorogenic ester molecules.[38] A full understanding of all of the contributors to non-photochemical release requires the thorough design of various model studies and constitutes the objective of future studies.

In summary, the extent of dye release was conveniently measured in real-time by fluorescence in situ. The resulting kinetics of dye release suggests that the release occurred through a mechanism triggered by the photolytic C–S cleavage of the TNB cage and subsequently by other non-photochemical mechanisms. Thus, measurements made shortly after UV activation represent the extent of drug released as triggered by the light stimulus, whereas measurements made over an extended incubation time represent release of drug collectively from a combination of photochemical and other mechanisms.

Conclusion

Major challenges facing the development of controlled drug release systems include the paucity of cage technologies that allow for active control and for gauging in situ how much drug is released from a cage system at a given dose.[11d,39] We have designed a novel TNB-based, dual arm cage with the unique ability to trigger light-controlled synchronous release of two payloads. Compared to existing bifunctional linkers,[11b,c,f,25,26,40] it offers synthetic convenience, an active mechanism for the control of payload release by light exposure, and rapid release kinetics comparable to an ONB cage system.[10b,13] Its practicality for fluorescence-based monitoring of drug release for in vitro cellular applications was investigated here by its conjugation with Taxol or doxorubicin, along with a conditionally fluorescent reporter. The conjugates exhibited a strong correlation between drug release and fluorescence measured in situ on a real-time basis. Furthermore, TNB conjugation was also able to maintain the drug compounds in a reduced cytotoxic state in the conjugated form, and the conjugates were taken up intracellularly at doses that were as cytotoxic as the unmodified drug upon UV activation.

We believe that this new strategy will make a broad impact on the advancement of fluorescence-based release control in a wide range of applications ranging from those involving small molecule drug–reporter conjugates to nanoparticulate delivery systems. This strategy offers important tools to the expanding field of photocaging,[2,6b,9] which has been applied not only to organic molecules but also to metal ions by using photolabile metal chelators,[41] such as acetal-based ONB,[42] which employs a similar fragmentation reaction at its acetal carbon. Finally, we believe that this TNB strategy has strong potential for use as a new platform for photocaging thiols, which can be used in the active control of cellular activities that are mediated by bioactive thiols including cysteine, among others. These applications range from the control of redox biology,[43] enzymes,[15,44] and ion channel permeability.[45] As discussed above, the values of $\Phi_{uncaging}$ that were determined for TNB-caged small thiols, including **1** and **2** (Table S1) are comparable to ONB-caged molecules[6b] and are supportive of the compatibility of such application. Future efforts will focus on extending and validating the scope of this TNB strategy in photocaged small molecules for chemical biology and in nanoscale systems designed for receptor-targeted anticancer therapeutic agents.

Acknowledgements

This work was supported by the Michigan Nanotechnology Institute for Medicine and Biological Sciences the National Cancer Institute (NCI) of the National Institutes of Health (NIH) (1R21A191428), and the British Council and Department for Business Innovation & Skills through the Global Innovation Initiative.

Keywords: antitumor agents · caged compounds · controlled release · dual arm cage · fluorescence reporter · photolysis

[1] J. W. Walker, J. A. McCray, G. P. Hess, *Biochemistry* **1986**, *25*, 1799 – 1805.
[2] G. Mayer, A. Heckel, *Angew. Chem. Int. Ed.* **2006**, *45*, 4900 – 4921; *Angew. Chem.* **2006**, *118*, 5020 – 5042.
[3] a) E. A. Lemke, D. Summerer, B. H. Geierstanger, S. M. Brittain, P. G. Schultz, *Nat. Chem. Biol.* **2007**, *3*, 769 – 772; b) B. N. Goguen, A. Aemissegger, B. Imperiali, *J. Am. Chem. Soc.* **2011**, *133*, 11038 – 11041.
[4] a) K. H. Link, Y. Shi, J. T. Koh, *J. Am. Chem. Soc.* **2005**, *127*, 13088 – 13089; b) P. Neveu, I. Aujard, C. Benbrahim, T. Le Saux, J.-F. Allemand, S. Vriz, D. Bensimon, L. Jullien, *Angew. Chem. Int. Ed.* **2008**, *47*, 3744 – 3746; *Angew. Chem.* **2008**, *120*, 3804 – 3806; c) X. Lu, S. S. Agasti, C. Vinegoni, P. Waterman, R. A. DePinho, R. Weissleder, *Bioconjugate Chem.* **2012**, *23*, 1945 – 1951.
[5] a) A. Momotake, N. Lindegger, E. Niggli, R. J. Barsotti, G. C. R. Ellis-Davies, *Nat. Methods* **2006**, *3*, 35 – 40; b) M. M. Mahmoodi, D. Abate-Pella, T. J. Pundsack, C. C. Palsuledesai, P. C. Goff, D. A. Blank, M. D. Distefano, *J. Am. Chem. Soc.* **2016**, *138*, 5848 – 5859.
[6] a) T. Furuta, S. S. H. Wang, J. L. Dantzker, T. M. Dore, W. J. Bybee, E. M. Callaway, W. Denk, R. Y. Tsien, *Proc. Natl. Acad. Sci. USA* **1999**, *96*, 1193 – 1200; b) P. Klán, T. Šolomek, C. G. Bochet, A. Blanc, R. Givens, M. Rubina, V. Popik, A. Kostikov, J. Wirz, *Chem. Rev.* **2013**, *113*, 119 – 191.
[7] Y. M. Li, J. Shi, R. Cai, X. Chen, Z. F. Luo, Q. X. Guo, *J. Photochem. Photobiol. A* **2010**, *211*, 129 – 134.
[8] A. P. Gorka, R. R. Nani, J. Zhu, S. Mackem, M. J. Schnermann, *J. Am. Chem. Soc.* **2014**, *136*, 14153 – 14159.
[9] M. M. Lerch, M. J. Hansen, G. M. van Dam, W. Szymanski, B. L. Feringa, *Angew. Chem. Int. Ed.* **2016**, *55*, 10978 – 10999; *Angew. Chem.* **2016**, *128*, 11140 – 11163.
[10] a) Y.-H. Chien, Y.-L. Chou, S.-W. Wang, S.-T. Hung, M.-C. Liau, Y.-J. Chao, C.-H. Su, C.-S. Yeh, *ACS Nano* **2013**, *7*, 8516 – 8528; b) S. K. Choi, T. Thomas, M. Li, A. Kotlyar, A. Desai, J. R. Baker, Jr., *Chem. Commun.* **2010**, *46*, 2632 – 2634; c) P. T. Wong, D. Chen, S. Tang, S. Yanik, M. Payne, J. Mukherjee, A. Coulter, K. Tang, K. Tao, K. Sun, J. R. Baker, Jr., S. K. Choi, *Small* **2015**, *11*, 6078 – 6090.
[11] a) S. Impellizzeri, B. McCaughan, J. F. Callan, F. M. Raymo, *J. Am. Chem. Soc.* **2012**, *134*, 2276 – 2283; b) S. Maiti, N. Park, J. H. Han, H. M. Jeon, J. H. Lee, S. Bhuniya, C. Kang, J. S. Kim, *J. Am. Chem. Soc.* **2013**, *135*, 4567 – 4572; c) Z. Yang, J. H. Lee, H. M. Jeon, J. H. Han, N. Park, Y. He, H. Lee, K. S. Hong, C. Kang, J. S. Kim, *J. Am. Chem. Soc.* **2013**, *135*, 11657 – 11662; d) G. M. Lanza, C. Moonen, J. R. Baker, E. Chang, Z. Cheng, P. Grodzinski, K. Ferrara, K. Hynynen, G. Kelloff, Y.-E. K. Lee, A. K. Patri, D. Sept, J. E. Schnitzer, B. J. Wood, M. Zhang, G. Zheng, K. Farahani, *Wiley Interdiscip. Rev. Nanomed. Nanobiotechnol.* **2014**, *6*, 1 – 14; e) S. S. Agasti, A. M. Laughney, R. H. Kohler, R. Weissleder, *Chem. Commun.* **2013**, *49*, 11050 – 11052; f) R. Weinstain, E. Segal, R. Satchi-Fainaro, D. Shabat, *Chem. Commun.* **2010**, *46*, 553 – 555.
[12] O. Redy-Keisar, S. Ferber, R. Satchi-Fainaro, D. Shabat, *ChemMedChem* **2015**, *10*, 999 – 1007.
[13] P. T. Wong, S. K. Choi, *Chem. Rev.* **2015**, *115*, 3388 – 3432.
[14] R. R. Anderson, J. A. Parrish, *J. Invest. Dermatol.* **1981**, *77*, 13 – 19.
[15] a) D. Abate-Pella, N. A. Zeliadt, J. D. Ochocki, J. K. Warmka, T. M. Dore, D. A. Blank, E. V. Wattenberg, M. D. Distefano, *ChemBioChem* **2012**, *13*, 1009 – 1016; b) D. P. Nguyen, M. Mahesh, S. J. Elsässer, S. M. Hancock, C. Uttamapinant, J. W. Chin, *J. Am. Chem. Soc.* **2014**, *136*, 2240 – 2243.
[16] a) M. A. Inlay, V. Choe, S. Bharathi, N. B. Fernhoff, J. R. Baker, I. L. Weissman, S. K. Choi, *Chem. Commun.* **2013**, *49*, 4971 – 4973; b) T. Faal, P. Wong, S. Tang, A. Coulter, Y. Chen, C. H. Tu, J. R. Baker, S. K. Choi, M. A. Inlay, *Mol. BioSyst.* **2015**, *11*, 783 – 790; c) D. K. Sinha, P. Neveu, N. Gagey, I. Aujard, T. L. Saux, C. Rampon, C. Gauron, K. Kawakami, C. Leucht, L. Bally-Cuif, M. Volovitch, D. Bensimon, L. Jullien, S. Vriz, *Zebrafish* **2010**, *7*, 199 – 204.
[17] P. K. Selbo, A. Weyergang, A. Høgset, O.-J. Norum, M. B. Berstad, M. Vikdal, K. Berg, *J. Controlled Release* **2010**, *148*, 2 – 12.
[18] a) S. K. Choi, T. P. Thomas, M.-H. Li, A. Desai, A. Kotlyar, J. R. Baker, *Photochem. Photobiol. Sci.* **2012**, *11*, 653 – 660; b) S. K. Choi, M. Verma, J. Silpe, R. E. Moody, K. Tang, J. J. Hanson, J. R. Baker, Jr., *Bioorg. Med. Chem.* **2012**, *20*, 1281 – 1290.
[19] M. M. Dcona, Q. Yu, J. A. Capobianco, M. C. T. Hartman, *Chem. Commun.* **2015**, *51*, 8477 – 8479.
[20] a) M. Noguchi, M. Skwarczynski, H. Prakash, S. Hirota, T. Kimura, Y. Hayashi, Y. Kiso, *Bioorg. Med. Chem.* **2008**, *16*, 5389 – 5397; b) M. Skwarczyn-

ski, M. Noguchi, S. Hirota, Y. Sohma, T. Kimura, Y. Hayashi, Y. Kiso, *Bioorg. Med. Chem. Lett.* **2006**, *16*, 4492 – 4496.
[21] S. S. Agasti, A. Chompoosor, C.-C. You, P. Ghosh, C. K. Kim, V. M. Rotello, *J. Am. Chem. Soc.* **2009**, *131*, 5728 – 5729.
[22] P. Wong, S. Tang, J. Mukherjee, K. Tang, K. Gam, D. Isham, C. Murat, R. Sun, J. R. Baker, S. K. Choi, *Chem. Commun.* **2016**, *52*, 10357 – 10360.
[23] a) Q. Lin, C. Bao, Y. Yang, Q. Liang, D. Zhang, S. Cheng, L. Zhu, *Adv. Mater.* **2013**, *25*, 1981 – 1986; b) Y. Yang, Q. Shao, R. Deng, C. Wang, X. Teng, K. Cheng, Z. Cheng, L. Huang, Z. Liu, X. Liu, B. Xing, *Angew. Chem. Int. Ed.* **2012**, *51*, 3125 – 3129; *Angew. Chem.* **2012**, *124*, 3179 – 3183.
[24] a) S. Karthik, B. N. Prashanth Kumar, M. Gangopadhyay, M. Mandal, N. D. P. Singh, *J. Mater. Chem. B* **2015**, *3*, 728 – 732; b) S. Yamazoe, Q. Liu, L. E. McQuade, A. Deiters, J. K. Chen, *Angew. Chem. Int. Ed.* **2014**, *53*, 10114 – 10118; *Angew. Chem.* **2014**, *126*, 10278 – 10282.
[25] S. Santra, C. Kaittanis, O. J. Santiesteban, J. M. Perez, *J. Am. Chem. Soc.* **2011**, *133*, 16680 – 16688.
[26] Y. Yuan, C.-J. Zhang, M. Gao, R. Zhang, B. Z. Tang, B. Liu, *Angew. Chem. Int. Ed.* **2015**, *54*, 1780 – 1786; *Angew. Chem.* **2015**, *127*, 1800 – 1806.
[27] K. C. Nicolaou, C. J. N. Mathison, T. Montagnon, *Angew. Chem. Int. Ed.* **2003**, *42*, 4077 – 4082; *Angew. Chem.* **2003**, *115*, 4211 – 4216.
[28] A. R. Katritzky, Y.-J. Xu, A. V. Vakulenko, A. L. Wilcox, K. R. Bley, *J. Org. Chem.* **2003**, *68*, 9100 – 9104.
[29] P. E. Dawson, M. J. Churchill, M. R. Ghadiri, S. B. H. Kent, *J. Am. Chem. Soc.* **1997**, *119*, 4325 – 4329.
[30] C. G. Hatchard, C. A. Parker, *Proc. R. Soc. London Ser. A* **1956**, *235*, 518 – 536.
[31] a) I. Ojima, *Acc. Chem. Res.* **2008**, *41*, 108 – 119; b) R. Labruère, A. Alouane, T. Le Saux, I. Aujard, P. Pelupessy, A. Gautier, S. Dubruille, F. Schmidt, L. Jullien, *Angew. Chem. Int. Ed.* **2012**, *51*, 9344 – 9347; *Angew. Chem.* **2012**, *124*, 9478 – 9481.
[32] Y. Hori, T. Norinobu, M. Sato, K. Arita, M. Shirakawa, K. Kikuchi, *J. Am. Chem. Soc.* **2013**, *135*, 12360 – 12365.
[33] I. Ojima, X. Geng, X. Wu, C. Qu, C. P. Borella, H. Xie, S. D. Wilhelm, B. A. Leece, L. M. Bartle, V. S. Goldmacher, R. V. J. Chari, *J. Med. Chem.* **2002**, *45*, 5620 – 5623.
[34] a) I. R. Vlahov, G. D. Vite, P. J. Kleindl, Y. Wang, H. K. R. Santhapuram, F. You, S. J. Howard, S.-H. Kim, F. F. Y. Lee, C. P. Leamon, *Bioorg. Med. Chem. Lett.* **2010**, *20*, 4578 – 4581; b) A. Kock, K. Zuwala, A. A. A. Smith, P. Ruiz-Sanchis, B. M. Wohl, M. Tolstrup, A. N. Zelikin, *Chem. Commun.* **2014**, *50*, 14498 – 14500.
[35] L. D. Lavis, T. J. Rutkoski, R. T. Raines, *Anal. Chem.* **2007**, *79*, 6775 – 6782.
[36] H. Staleva, J. Komenda, M. K. Shukla, V. Šlouf, R. Kaňa, T. Polívka, R. Sobotka, *Nat. Chem. Biol.* **2015**, *11*, 287 – 291.
[37] J. M. Ndungu, Y. J. Lu, S. Zhu, C. Yang, X. Wang, G. Chen, D. M. Shin, J. P. Snyder, M. Shoji, A. Sun, *J. Med. Chem.* **2010**, *53*, 3127 – 3132.
[38] A. Laurent, F. Debart, N. Lamb, B. Rayner, *Bioconjugate Chem.* **1997**, *8*, 856 – 861.
[39] T. Lammers, S. Aime, W. E. Hennink, G. Storm, F. Kiessling, *Acc. Chem. Res.* **2011**, *44*, 1029 – 1038.
[40] S. Bhuniya, S. Maiti, E.-J. Kim, H. Lee, J. L. Sessler, K. S. Hong, J. S. Kim, *Angew. Chem. Int. Ed.* **2014**, *53*, 4469 – 4474; *Angew. Chem.* **2014**, *126*, 4558 – 4563.
[41] a) G. C. R. Ellis-Davies, *Chem. Rev.* **2008**, *108*, 1603 – 1613; b) A. S. R. Adams, R. Y. Tsien, *Annu. Rev. Physiol.* **1993**, *55*, 755 – 784.
[42] G. C. R. Ellis-Davies, J. H. Kaplan, *J. Org. Chem.* **1988**, *53*, 1966 – 1969.
[43] L. B. Poole, *Free Radical Biol. Med.* **2015**, *80*, 148 – 157.
[44] J. H. Qi, L. Zhang, J. Wang, M. Lu, X. M. Wang, Z. J. Jin, *Cell Res.* **1996**, *6*, 47 – 53.
[45] D. Alansary, B. Schmidt, K. Dörr, I. Bogeski, H. Rieger, A. Kless, B. A. Niemeyer, *Sci. Rep.* **2016**, *6*, 33347.

Manuscript received: September 7, 2016
Accepted Article published: November 7, 2016
Final Article published: November 30, 2016